New Low Band Gap Polymers: Control of Optical and Electronic Properties in near Infrared Absorbing π-Conjugated Polysquaraines

J. Eldo and A. Ajayaghosh*

Photochemistry Research Unit, Regional Research Laboratory, CSIR, Trivandrum 695 019, India

Received August 7, 2001. Revised Manuscript Received October 2, 2001

A novel approach to design extremely low band gap polysquaraines with intense near-infrared (NIR) absorption and high intrinsic conductivity is described. Feasibility of the new strategy is illustrated by an A-B type copolymerization of squaric acid and 1,4-dialkoxy-divinylbenzene-bridged bispyrroles, which resulted in zwitterionic polysquaraines with resonance stabilized quinoid structures. Incorporation of an electron donating conjugated moiety between each squaraine dye repeating unit has a dramatic influence on the optical and electronic properties of the resulting polysquaraines due to an enhanced donor−acceptor−donor interaction. The solution UV−Vis−NIR absorption maxima of the new polymers, between 772 and 1040 nm with ground-state onset absorptions ranging from 1140 to 1300 nm, is unusual for conjugated polymers and is a signature of their low band gaps. The band gaps of these polymers are around 1 eV with the lowest value of 0.79 eV for **6a**. The intrinsic conductivities of these polymers could be modulated between 10^{-7}−10^{-4} S/cm by varying the length of the alkyl side chains. This is in agreement with the molecular packing data obtained from the X-ray analysis that revealed an interdigitated arrangement of the polymer chains. The solubility inducing alkyl side chains play a decisive role in the molecular packing, which control the optical band gap and conductivity of the reported polysquaraines. This is one of the simplest strategies for the synthesis of NIR absorbing conjugated polymers with extremely low band gaps that are soluble and intrinsically semiconducting.

Introduction

The discovery of electrical conductivity in doped polyacetylene by Shirakawa et al. has stimulated enormous scientific and technological activities in the area of π-conjugated polymers.[1] Doping of these polymers to make them electrically conducting at the expense of some of the desired properties such as solubility and processability has limited their applications to a large extent. Efforts to overcome some of these limitations were made in recent years by synthesizing intrinsically semiconducting low band gap (E_g) polymers.[2] Since optical absorption in π-conjugated systems plays a key role in determining the HOMO−LUMO energy gap and the intrinsic electronic properties, control of these parameters by molecular engineering is of great significance. In several cases, this has been achieved by strategies such as rigidification of the polymer backbone and enhancing the polymer's nonclassical quinoid character.[3,4] Twist inhibition between consecutive repeating units of conjugated polymers using irreversible ladder-type bonds,[5] and the use of zwitterionic structures involving alternating π-bonds[6] or reversible noncovalent linkages,[7] are shown to be effective in the lowering of E_g in conjugated polymers. An entirely different approach is the use of a combination of donor and acceptor monomers in regular intervals of repeating units, invoking strong charge-transfer interactions.[8] However, this

* To whom correspondence should be addressed. Fax: +91 471 490 186, E-mail: aajayaghosh@rediffmail.com.

(1) (a) Shirakawa, H.; Louis, E. J.; MacDiarmid, A. G.; Chiang, C. K.; Heeger, A. J. *J. Chem. Soc., Chem. Commun*. **1977**, 578. (b) Chiang, C. K.; Fischer, C. R.; Park, Y. W.; Heeger, A. J.; Shirakawa, H.; Louis, E. J.; Gau, S. C; MacDiarmid, A. G. *Phys. Rev. Lett*. **1977**, *39*, 1098. (c) Chiang, C. K.; Druy, M. A.; Gau, S. C.; Heeger, A. J.; Louis, E. J.; MacDiarmid, A. G.; Park, Y. W.; Shirakawa, H. *J. Am. Chem. Soc.* **1978**, *100*, 1013.

(2) (a) Hanack, M.; Schmid, U.; Echinger, S.; Teichert, F.; Hieber, J. *Synthesis* **1993**, 634. (b) Roncali, J. *Chem. Rev.* **1997**, *97*, 173.

(3) (a) Ferraris, J. P.; Bravo, A.; Kim, W.; Hrncir, D. C. *J. Chem. Soc., Chem. Commun.* **1994**, 991. (b) Roncali, J.; Thobie-Gautier, C.; Elandaloussi, E. H.; Frère, F. *J. Chem. Soc., Chem. Commun*. **1994**, 2249. (c) Roncali, J.; Thobie-Gautier, C. *Adv. Mater*. **1994**, *6*, 846.

(4) (a) Bredas, J. L. *J. Chem. Phys*. **1985**, *82*, 3808. (b) Wudl, F.; Kobayashi, M.; Heeger, A. J. *J. Org. Chem*. **1984**, *49*, 3382. (c) Jenekhe, S. A. *Nature* **1986**, *322*, 345. (d) Hanack, M.; Hieber, G.; Mangold, K.-M.; Ritter, H.; Rohrig, U.; Schmid, U.; *Synth. Met*. **1993**, *55*−*57*, 827. (e) Echinger, S.; Schmid, U.; Teichert, F.; Hieber, J.; Ritter, R.; Hanack, M. *Synth. Met*. **1993**, *61*, 163. (f) Aota, H.; Reikan, T.; Matsumoto, A.; Kamachi, M. *Chem. Lett*. **1997**, 527. (g) Aota, H.; Reikan, T.; Matsumoto, A.; Kamachi, M. *Chem. Lett*. **1998**, 335.

(5) (a) Overberger, C. G.; Moore, J. A. *Adv. Polym. Sci*. **1970**, *7*, 113. (b) Godt, A.; Schlüter, A.-D. *Adv. Mater*. **1991**, *3*, 497. (c) Yu, L.; Dalton, L. R. *Macromolecules* **1990**, *23*, 3439. (d) Kertesz, M.; Hong, S. Y. *Macromolecules* **1992**, *25*, 5424. (e) Scherf, U.; Müllen, K. *Synthesis* **1992**, 23. (f) Lamba, J. J. S.; Tour, J. M. *J. Am. Chem. Soc.* **1994**, *116*, 11723. (g) Zhang, Q. T.; Tour, J. M. *J. Am. Chem. Soc.* **1997**, *119*, 9624. (h) Yao, Y.; Lamba, J. J. S.; Tour, J. M. *J. Am. Chem. Soc.* **1998**, *120*, 2805. (i) Goldfinger, M. B.; Swager, T. M. *J. Am. Chem. Soc.* **1994**, *116*, 7895. (j) Nuckolls, C.; Katz, T. J.; Castellanos, L. *J. Am. Chem. Soc.* **1996**, *118*, 3767.

(6) (a) Brockmann, T. W.; Tour J. M. *J. Am. Chem. Soc*. **1994**, *116*, 7435. (b) Brockmann, T. W.; Tour J. M. *J. Am. Chem. Soc.* **1995**, *117*, 4437.

10.1021/cm0107225 CCC: $22.00
Published on Web 12/05/2001

strategy has not been very successful in the designing of polymers with an E_g below 1 eV. Even though several oxidative polymerization strategies are available for the synthesis of low E_g polymers, a reasonably viable nonoxidative polymerization pathway to intrinsically semiconducting polymers and control of their optical and electronic properties remains important.[9]

Inspired by the challenge of designing low E_g polymers with intense NIR absorption, we focused our attention on a novel class of conjugated polymers derived from squaraine dyes. There are several reports in the literature pertaining to the studies of polysquaraines in anticipation of low HOMO−LUMO separation due to a strong donor−acceptor−donor interaction.[10] We have been exploring the use of pyrrole derivatives with a view to designing squaraine dye based low E_g polymers[11] and polymer-based chemosensors.[12] However, these polymers absorb below 700 nm, and their band gaps are relatively high. This is contrary to the recent theoretical prediction that squaraine dyes can be used to construct intrinsically semiconducting polymers with extremely small band gaps.[13] As a result of our continued effort in this area, recently we have reported a novel strategy toward the synthesis of low E_g polysquaraines with intense NIR absorption.[14,15] The strategy involves a nonoxidative A-B type polycondensation of logically selected molecular components via the in situ generation of a squaraine dye at well-defined positions of a conjugated backbone, which is capable of electronically communicating with each repeating segment of the polymer with the aid of a strongly electron-donating moiety. In the present paper, detailed studies on the synthesis and characterization of a number of NIR absorbing low E_g polysquaraines and the role of alkoxy side chains to control their optical properties and electronic conduction are described.

Experimental Section

General. Unless otherwise stated, all starting materials and reagents were purchased from commercial suppliers and used without further purification. All solvents were purified and dried by standard methods prior to use. Melting points were determined with a Mel-Temp-II melting point apparatus and are uncorrected. The mass spectra were recorded on a Hewlett-Packard mass spectrometer model 5791, attached to 5890 series II gas chromatography setup, attached with an OV 101 or on MP−FFAP capillary column, and a FID detector. ^{1}H and ^{13}C NMR spectra were measured on a 300 MHz Bruker Avance DPX spectrometer. FT-IR spectra were recorded on a Nicolet Impact 400D infrared spectrophotometer. Elemental analyses were done using a Perkin-Elmer series-II 2400 CHN analyzer. High-resolution mass spectra were recorded on a JEOL JM AX 505 HA mass spectrometer at the Radiation Laboratory, University of Notre Dame.

The UV−Vis−NIR spectra were recorded on a Shimadzu UV-3101 PC NIR Scanning spectrophotometer. The emission spectra were measured on a SPEX-Fluorolog F112X spectrofluorimeter. The molecular weights were determined on a Waters GPC system equipped with a refractive index detector and Waters columns HR-1, HR-2, and HR-3, which are connected in series. THF was used as eluent at a flow rate of 1 mL/min. Calibration was done with standard polystyrenes. Cyclic voltammetry was performed on a BAS CV50W cyclic voltammeter using tetrabutylammonium hexafluorophosphate as supporting electrolyte in dichloromethane. A standard three-electrode configuration was used with a glassy carbon as working electrode, a Pt wire as auxiliary electrode, and a silver wire as reference electrode. The potentials were calibrated against saturated calomel electrode (SCE) unless otherwise stated. Thermogravimetric analysis of **6a**−**g** was carried out on a Shimadzu TGA-50H thermal analyzer under nitrogen at a heating rate of 20 °C/min. X-ray diffraction studies were performed on a Phillips diffractometer using Ni filtered Cu Kα radiation. SEM pictures were obtained on a JEOL 5600 LV scanning electron microscope with an accelerating voltage of 10 kV. Polymer films for the SEM analysis were prepared from their chloroform solutions and coated with gold by ion sputtering. Intrinsic conductivities were measured using pressed rectangular pellets (4 × 20 mm) on a Kiethley model 6517A electrometer. Doped conductivities were measured after exposing the polymers in an iodine chamber until a constant weight was obtained in each case.

Preparation of Bispyrroles 5a−g. General Procedure. A suspension of sodium hydride (30 mmol) in THF was added slowly to a solution of the corresponding 2,5-bis (alkyloxy)-1,4-bis (benzyl) phosphonate (5 mmol) and the respective *N*-alkylpyrrole-2-carboxaldehyde (10 mmol) in THF. After the sample was refluxed for 10 h, the highly fluorescent reaction mixture was cooled, and THF was removed under reduced pressure to give a solid residue. This residue was suspended in water and extracted with dichloromethane. The organic layer was washed with brine, dried over $MgSO_4$, and concentrated to give a crude product, which was further purified by several precipitations by adding methanol to a dichloromethane solution. The spectral data of **5a**−**g** after recrystallization from a mixture of dichloromethane/petroleum ether were in agreement with their structures as illustrated below.

***(E,E)*-1,4-Bis[2-(1-methylpyrrol-2-yl)vinyl]-2,5-dibutoxybenzene (5a).** Yield 63%; mp 140−142 °C; IR (KBr) ν_{max} 2949, 2868, 1462, 1417, 1327, 1197, 1039, 1012, 954, 707 cm^{-1}; ^{1}H NMR ($CDCl_3$) δ 7.08 (d, J = 16.26 Hz, 2H), 7.00 (d, J = 16.30

(7) (a) Marsella, M. J.; Swager, T. M. *J. Am. Chem. Soc.* **1993**, *115*, 12214. (b) McCullough, R. D.; Williams, S. P. *J. Am. Chem. Soc.* **1993**, *115*, 11608. (c) McCullough, R. D.; Williams, S. P. *Chem. Mater.* **1995**, *7*, 2001. (d) Jenekhe, S. A.; Osaheni, J. A. *Macromolecules* **1992**, *25*, 5828. (e) Tarkka, R. M.; Zhang, X.; Jenekhe, S. A. *J. Am. Chem. Soc.* **1996**, *118*, 9438. (f) van Mullekom, H. A. M.; Vekemans, J. A. J. M.; Meijer, E. W. *Chem. Commun.* **1996**, 2163. (g) Delnoye, D. A. P.; Sijbesma, R. P.; Vekemans, J. A. J. M.; Meijer, E. W. *J. Am. Chem. Soc.* **1996**, *118*, 8717.

(8) Donor−acceptor strategies reported earlier are not very successful in providing extremely low E_g polymers. See (a) Yamamoto, T.; Zhou, Z.-h.; Kanbara, M.; Kizu, K.; Maruyama, T.; Nakamura, Y.; Fukuda, T.; Lee, B.-L.; Ooba, N.; Tomaru, S.; Kurihara, T.; Kaino, T.; Kubota, K.; Sasaki, S. *J. Am. Chem. Soc.* **1996**, *118*, 10389. (b) Van Mullekom, Vekemans, J. A. J. M.; Meijer, E. W. *Chem. Eur. J.* **1998**, *4*, 1235. (c) Zhang, T. Q.; Tour, J. M. *J. Am. Chem. Soc.* **1997**, *119*, 5065. (d) Zhang, T. Q.; Tour, J. M. *J. Am. Chem. Soc.* **1997**, *120*, 5355.

(9) (a) Pomerantz, M.; Chaloner-Gill, B.; Harding, L. O.; Tseng, J. J.; Pomerantz, W. J. *Synth. Met.* **1993**, *55*−*57*, 960. (b) Tanaka, S.; Yamashita, Y. *Synth. Met.* **1995**, *69*, 599. (c) Karikomi, M.; Kitamura, C.; Tanaka, S.; Yamashita, Y. *J. Am. Chem. Soc.* **1995**, *117*, 6791. (d) Tanaka, S.; Yamashita, Y. *Synth. Met.* **1997**, *84*, 229. (e) Akoudad, S.; Roncali, J. *Chem. Commun.* **1998**, 2081.

(10) (a) Treibs, A.; Jacob, K. *Angew. Chem., Int. Ed. Engl.* **1965**, *4*, 694. (b) Hall, H. K., Jr.; Chen. Y. −Y. *Polym. Bull.* **1986**, *16*, 419−425. (c) Havinga, E. E.; ten Hoeve, W.; Wynberg, H. *Polym. Bull.* **1992**, *29*, 119. (d) Havinga, E. E.; ten Hoeve, W.; Wynberg, H. *Synth. Met.* **1993**, *55*−*57*, 299. (e) Havinga, E. E.; Pomp, A.; ten Hoeve, W.; Wynberg, W. *Synth. Met.* **1995**, *69*, 581. (f) Lynch, D. E.; Geissler, U.; Kwiatkowski, J.; Whittaker, A. K. *Polym. Bull.* **1997**, *38*, 493. (g) Lynch, D. E.; Geissler, U.; Peterson, I. R.; Floersheimer, M.; Terbrack, R.; Chi, L. F.; Fuchs, H.; Calos, N. J.; Wood, B.; Kennard, C. H. L.; Langley, G. J. *J. Chem. Soc., Perkin Trans. 2*, **1997**, 827.

(11) (a) Ajayaghosh, A.; Chenthamarakshan, C. R.; Das, S.; George, M. V. *Chem. Mater.* **1997**, *9*, 644. (b) Chenthamarakshan, C. R.; Ajayaghosh, A. *Chem. Mater.* **1998**, *10*, 1657. (c) Chenthamarakshan, C. R.; Eldo, J.; Ajayaghosh, A. *Macromolecules* **1999**, *32*, 251.

(12) (a) Chenthamarakshan, C. R.; Ajayaghosh, A. *Tetrahedron Lett.* **1998**, *39*, 1795. (b) Chenthamarakshan, C. R.; Eldo, J.; Ajayaghosh, A. *Macromolecules* **1999**, *32*, 5846.

(13) (a) Brocks, G. *J. Chem. Phys.* **1995**, *102*, 2522. (b) Brocks, G.; Tol, A. *J. Phys. Chem.* **1996**, *100*, 1838.

(14) Ajayaghosh, A.; Eldo, J. *Org. Lett.* **2001**, *3*, 2595.

(15) Polymers with intense NIR sensitivity are important as dyes for optical data storage. However, π-conjugated polymers with intense NIR absorption are rare. See (a) Zollinger, H. *Color Chemistry*; VCH: New York, 1991. (b) Fabian, J.; Nakazumi, H.; Matsuoka, M. *Chem. Rev.* **1992**, *92*, 1197.

Hz, 2H), 6.91 (s, 2H), 6.56 (s, 2H), 6.42 (m, 2H), 6.09 (t, J = 2.75 Hz, 2H), 3.96 (t, J = 6.27 Hz, 4H), 3.63 (s, 6H), 1.74 (t, 4H), 1.50 (m, 4H), 0.94 (t, J = 7.31 Hz, 6H); ^{13}C NMR ($CDCl_3$) δ 150.93, 132.87, 126.56, 123.44, 121.46, 117.56, 110.95, 108.23, 106.63, 69.12, 34.15, 31.66, 19.47, 13.91; HRMS calcd for $C_{28}H_{36}N_2O_2$ (M^+): 432.2777, found 432.2770.

(*E,E*)-1,4-Bis[2-(1-methylpyrrol-2-yl)vinyl]-2,5-dioctyloxybenzene (5b). Yield 72%; mp 108−110 °C; IR (KBr) ν_{max} 2920, 2851, 1507, 1413, 1310, 1227, 1202, 1059, 1031, 957, 707 cm^{-1}; ^{1}H NMR ($CDCl_3$) δ 7.14 (d, J = 16.30 Hz, 2H), 7.05 (d, J = 16.30 Hz, 2H), 6.98 (s, 2H), 6.62 (s, 2H), 6.48 (m, 2H), 6.15 (t, J = 2.68 Hz, 2H), 4.01 (t, J = 6.33 Hz, 4H), 3.69 (s, 6H), 1.84 (m, 4H), 1.54 (m, 4H), 1.29 (m, 16H), 0.88 (t, J = 6.75 Hz, 6H); ^{13}C NMR ($CDCl_3$) δ 150.96, 132.88, 126.61, 123.45, 121.44, 117.53, 110.96, 108.25, 106.68, 69.53, 34.20, 31.84, 29.65, 29.45, 29.30, 26.31, 22.67, 14.10; HRMS calcd for $C_{36}H_{52}N_2O_2$ (M^+): 544.4029, found 544.4041; Anal. calcd for $C_{36}H_{52}N_2O_2$: C, 79.36; H, 9.62; N, 5.14. Found: C, 79.10; H, 9.80; N, 5.10.

(*E,E*)-1,4-Bis[2-(1-methylpyrrol-2-yl)vinyl]-2,5-didodecyloxybenzene (5c). Yield 80%; mp 79−80 °C; IR (KBr) ν_{max} 2921, 2851, 1463, 1310, 1227, 1205, 1065, 960, 697 cm^{-1}; ^{1}H NMR ($CDCl_3$) δ 7.14 (d, J = 16.28 Hz, 2H), 7.05 (d, J = 16.28 Hz, 2H), 6.97 (s, 2H), 6.63 (s, 2H), 6.48 (m, 2H), 6.15 (t, J = 2.82 Hz, 2H), 4.01 (t, J = 6.26 Hz, 4H), 3.69 (s, 6H), 1.84 (m, 4H), 1.51 (m, 4H), 1.26 (m, 32H), 0.88 (t, J = 6.70 Hz, 6H); ^{13}C NMR ($CDCl_3$) δ 150.95, 132.87, 126.60, 123.44, 121.44, 117.53, 110.96, 108.24, 106.68, 69.52, 34.19, 31.90, 29.63, 29.49, 29.34, 26.30, 22.67, 14.10; HRMS calcd for $C_{44}H_{68}N_2O_2$ (M^+): 656.5281, found 656.5263.

(*E,E*)-1,4-Bis[2-(1-dodecylpyrrol-2-yl)vinyl]-2,5-dimethoxybenzene (5d). Yield 70%; mp 85−86 °C; IR (KBr) ν_{max} 2927, 2857, 1543, 1496, 1461, 1336, 1288, 1206, 1046, 955 cm^{-1}; ^{1}H NMR ($CDCl_3$) δ 7.03 (d, J = 16.12 Hz, 2H), 6.91 (d, J = 16.3 Hz, 2H), 6.89 (s, 2H), 6.56 (s, 2H), 6.40 (m, 2H), 6.05 (t, J = 3.13 Hz, 2H), 3.88 (t, J = 7.16 Hz, 4H), 3.80 (s, 6H), 1.69 (m, 4H), 1.17−1.25 (m, 36H), 0.80 (t, J = 6.82 Hz, 6H); ^{13}C NMR ($CDCl_3$) δ 151.40, 131.85, 126.53, 122.40, 120.79, 117.71, 109.56, 108.26, 106.82, 56.34, 47.08, 31.91, 31.59, 29.62, 29.37, 29.31, 26.91, 22.74, 14.12; HRMS calcd for $C_{44}H_{68}N_2O_2$ (M^+): 656.5281, found 656.5256.

(*E,E*)-1,4-Bis[2-(1-dodecylpyrrol-2-yl)vinyl]-2,5-dibutoxybenzene (5e). Yield 60%; mp 79−80 °C; IR (KBr) ν_{max} 2922, 2850, 1698, 1649, 1541, 1521, 1442, 1339, 1227, 1080, 958 cm^{-1}; ^{1}H NMR ($CDCl_3$) δ 7.12 (d, J = 16.3 Hz, 2H), 7.06 (d, J = 16.3 Hz, 2H), 6.96 (s, 2H), 6.67 (s, 2H), 6.48 (m, 2H), 6.16 (t, J = 2.97 Hz, 2H), 4.02 (t, J = 6.3 Hz, 4H), 3.96 (t, J = 6.7 Hz, 4H), 1.76−1.86 (m, 8H), 1.52−1.62 (m, 8H), 1.24−1.29 (m, 32H), 1.00 (t, J = 7.16 Hz, 6H), 0.87 (t, J = 5.69 Hz, 6H); ^{13}C NMR ($CDCl_3$) δ 150.94, 132.13, 126.59, 122.41, 121.47, 117.81, 111.20, 108.15, 106.47, 69.12, 47.10, 31.89, 31.68, 31.57, 29.58, 29.31, 29.27, 26.87, 22.66, 19.47, 14.08, 13.93; HRMS calcd for $C_{50}H_{80}N_2O_2$ (M^+): 740.6220, found 740.6212.

(*E,E*)-1,4-Bis[2-(1-dodecylpyrrol-2-yl)vinyl]-2,5-dioctyloxybenzene (5f). Yield 64%, mp 91−92 °C; IR (KBr) ν_{max} 2931, 2863, 1656, 1628, 1509, 1490, 1392, 1360, 1295, 1094, 962 cm^{-1}; ^{1}H NMR ($CDCl_3$) δ 7.09 (d, J = 15.56 Hz, 2H), 7.06 (d, J = 15.66 Hz, 2H), 6.95 (s, 2H), 6.66 (m, 2H) 6.48 (m, 2H), 6.14 (t, J = 2.94 Hz, 2H), 4.01 (t, J = 7.0 Hz, 4H), 3.95 (t, J = 6.63 Hz, 4H), 1.79 (m, 8H), 1.24−1.48 (m, 56H), 0.87 (t, J = 6.7 Hz, 12H); ^{13}C NMR (75.4 MHz, $CDCl_3$), δ 150.91, 132.09, 126.54, 122.40, 121.43, 117.79, 111.19, 108.13, 106.44, 69.45, 47.08, 31.90, 31.57, 29.64, 29.45, 29.34, 29.28, 26.87, 26.28, 22.67, 14.10; HRMS calcd for $C_{58}H_{96}N_2O_2$ (M^+): 852.7472, found 852.7468.

(*E,E*)-1,4-Bis[2-(1-dodecylpyrrol-2-yl)vinyl]-2,5-didodecyloxybenzene (5g). Yield 68%; mp 88−89 °C; IR (KBr) ν_{max} 2929, 2856, 1622, 1508, 1468, 1388, 1299, 1230, 1037, 960 cm^{-1}; ^{1}H NMR ($CDCl_3$) δ 7.09 (d, J = 16.0 Hz, 2H), 7.08 (d, J = 16.0 Hz, 2H), 6.95 (s, 2H), 6.67 (s, 2H), 6.48 (m, 2H), 6.15 (t, J = 2.9 Hz, 2H), 4.01 (t, J = 7.0 Hz, 4H), 3.95 (t, J = 7.14 Hz, 4H), 1.76−1.84 (m, 8H), 1.51 (m, 4H), 1.21−1.26 (m, 68 H), 0.87 (t, J = 6.96 Hz, 12H); ^{13}C NMR ($CDCl_3$) δ 150.94, 132.12, 126.58, 122.41, 121.45, 117.8, 111.23, 108.14, 106.48, 69.49, 47.10, 31.91, 31.57, 29.65, 29.34, 29.29, 26.88, 26.28, 22.67, 14.1; HRMS calcd for $C_{66}H_{112}N_2O_2$ (M^+): 964.8724, found 964.8707

Preparation of Polysquaraines 6a−g. The bispyrroles **5a−g (**0.15 mmol**)** and squaric acid (0.15 mmol) in butanol/benzene (1:3, 50 mL) were refluxed for 16−20 h under azeotropic removal of water. The reaction mixture was cooled and filtered, and the filtrate was concentrated under reduced pressure. The resultant dark green residue was dissolved in dichloromethane, and the product was precipitated with hexane and washed thoroughly with diethyl ether and methanol. After three reprecipitations and washing with hexane, diethyl ether, and methanol, **6a−g** were obtained in 69−80% yields. Polymers **6f** and **6g** having maximum solubility in $CDCl_3$ were characterized by ^{1}H NMR, IR, and elemental analyses, whereas polymers **6a−e** were characterized by IR and elemental analyses.

6a: Yield 71%, IR (KBr) ν_{max} 2950, 1612, 1493, 1342, 1274, 1101, 953 cm^{-1}; Anal. calcd for $(C_{32}H_{34}N_2O_4{\cdot}H_2O)_n$: C, 72.74; H, 6.86; N, 5.3. Found: C, 72.92; H, 6.86; N, 5.57.

6b: Yield 72%, IR (KBr) ν_{max} 2901, 1620, 1438, 1351, 1283, 1101, 946 cm^{-1}; Anal. calcd for $(C_{40}H_{50}N_2O_4{\cdot}H_2O)_n$: C, 74.96; H, 8.17; N, 4.37. Found: C, 75.32; H, 8.21; N, 4.51.

6c: Yield 80%, IR (KBr) ν_{max} 2923, 1621, 1445, 1348, 1278, 1090, 944 cm^{-1}; Anal. calcd for $(C_{48}H_{66}N_2O_4{\cdot}H_2O)_n$: C, 76.56; H, 9.1; N, 3.72. Found: C, 76.81; H, 9.2; N, 4.1.

6d: Yield 70%, IR (KBr) ν_{max} 2923, 2860, 1621, 1486, 1359, 1291, 1088, 950 cm^{-1}; Anal. calcd for $(C_{48}H_{66}N_2O_4{\cdot}H_2O)_n$: C, 76.56; H, 9.1; N, 3.72. Found: C, 76.40; H, 9.37; N, 3.66.

6e: Yield 80%, IR (KBr) ν_{max} 2917, 1629, 1463, 1350, 1297, 1097, 945 cm^{-1}; Anal. calcd for $(C_{54}H_{78}N_2O_4{\cdot}H_2O)_n$: C, 77.46; H, 9.63; N, 3.34. Found: C, 77.00; H, 10.26; N, 3.07.

6f: Yield 69%, IR (KBr) ν_{max} 2921, 2859, 1620, 1489, 1359, 1284, 1091, 954 cm^{-1}; ^{1}H NMR ($CDCl_3$) δ 7.5−7.8 (m, broad, vinylic), 6.8−7.01 (m, broad, aromatic), 4.78 (s, broad, NCH_2), 3.62−3.92 (m, NCH_2 and OCH_2), 1.22−1.86 (m, CH_2, 64H), 0.84 (t, CH_3, 12H); ^{13}CNMR ($CDCl_3$, 75.4 MHz) δ 177.79, 161.76, 151.9, 130.5, 113.92, 113.58, 69.33, 46.71, 31.94, 29.70, 29.46, 29.39, 26.53, 26.28, 22.7, 14.12; Anal. calcd for $(C_{62}H_{94}N_2O_4{\cdot}H_2O)_n$: C, 78.43; H, 10.19; N, 2.95. Found: C, 77.72; H, 10.31; N, 2.77.

6g: Yield 75%, IR (KBr) ν_{max} 2923, 1622 1434, 1360, 1292, 1090, 954 cm^{-1}; ^{1}H NMR ($CDCl_3$) δ 7.48−7.8 (m, broad, vinylic), 6.8−7.0 (m, broad, aromatic), 4.75 (s, broad, NCH_2), 3.6−3.91 (m, NCH_2 & OCH_2), 1.22−1.86 (m, CH_2, 80H), 0.84 (t, CH_3, 12H); ^{13}CNMR ($CDCl_3$, 75.4 MHz) δ 177.79, 161.76, 151.9, 130.5, 113.92, 113.58, 69.33, 46.71, 31.94, 31.56, 29.70, 29.46, 29.39, 26.53, 26.28, 22.7, 14.12; Anal. calcd for $(C_{70}H_{110}N_2O_4{\cdot}H_2O)_n$: C, 79.19; H, 10.63; N, 2.63. Found: C, 78.42; H, 10.56; N, 2.56.

Results and Discussion

Synthesis of polysquaraines **6a−g** was achieved by a multistep strategy as shown in Scheme 1. The hydroquinone **1** on reaction with the respective alkyl bromide gave the dialkoxybenzene derivatives **2a−d,** as per a reported procedure.[16] The bisbromomethyl derivatives **3a−d** were obtained in high yields using paraformaldehyde and HBr in acetic acid via a modified procedure using sonication. Arbuzov reaction of **3a−d** with triethyl phosphite gave the corresponding phosphonates **4a−d** in 70−80% yield.[17] Wittig−Horner−Emmons reaction of **4a−d** with the appropriate *N*-alkylpyrrole-2-carboxaldehydes gave the bispyrroles **5a−g** in 60−80% yields.[18] They showed absorption maxima around 400−420 nm due to $\pi-\pi^*$ transition and strong fluo-

(16) (a) Chen, S.-A.; Chang, E.-C. *Macromolecules* **1998**, *31*, 4899. (b) Wang, B.; Wasielewski, M. R. *J. Am. Chem. Soc.* **1997**, *119*, 12.
(17) Arbuzov, B. A. *Pure Appl. Chem*. **1964**, *9*, 307.
(18) Eldo, J.; Arunkumar, E.; Ajayaghosh, A. *Tetrahedron Lett.* **2000**, *41*, 6241.

Scheme 1

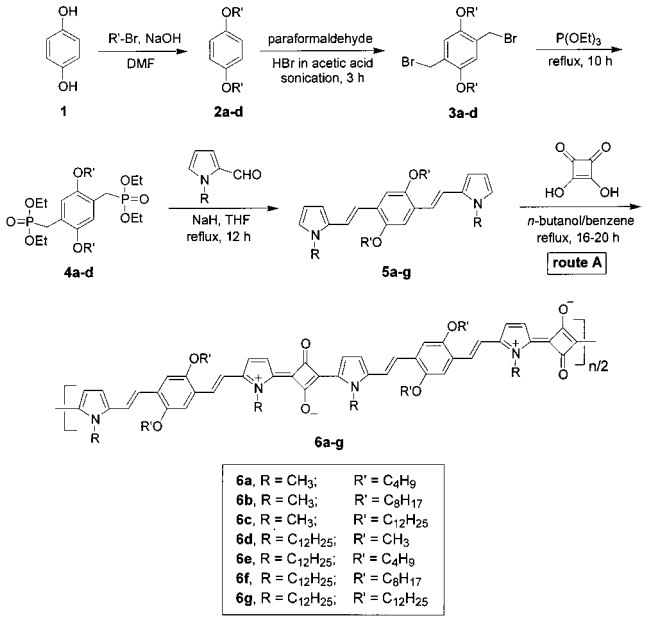

Scheme 2

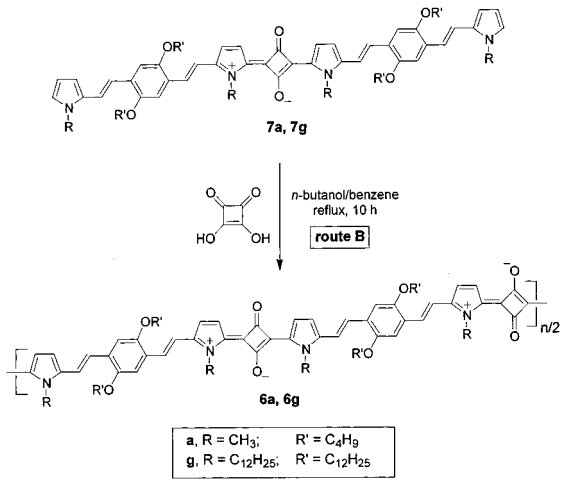

rescence emission around 470−480 nm with relatively high quantum yields (Φ_F = 0.38−0.41 in toluene). Structures of **5a**−**g** were confirmed by NMR and high-resolution mass spectral analysis. The all-trans configurations of **5a**−**g** were clear from the observed coupling constants (J = 16 Hz) in their ^{1}H NMR spectra.

Polysquaraines **6a**−**g** were prepared by the A−B type polycondensation of bispyrroles **5a**−**g** with squaric acid (1:1 stoichiometry) in a mixture (1:3) of *n*-butanol-benzene (route A), following the standard procedure of squaraine dye synthesis.[19] The reaction conditions were optimized by changing the dilution of the reactants and composition of the solvent mixtures. Progress of the polycondensation was monitored in each case by the changes in the absorption spectra of the reaction mixtures at different time intervals. For example, reaction of squaric acid with **5a** having shortest alkyl side chains resulted in a green solution, which absorbs around 762 nm, with the slow formation of two new shoulders, around 871 and 1041 nm (see Supporting Information). After 10 h of refluxing, the intensity of the 871 nm band became predominant. Within this period, the absorption of the starting bispyrrole **5a** at 411 nm almost disappeared, and the spectrum of **6a** became very broad with vibronic features. In the case of polysquaraines with long alkyl side chains, the initially formed strong absorption peak at 760 nm was subsequently changed into two new bands absorbing at 865 and 993 nm. (See Supporting Information.) After 10 h of refluxing, the 760 nm band was considerably weakened, and the 993 nm band became predominant. In all cases under investigation, the final products were isolated in 69−80% yields after 16−20 h of reaction, followed by repeated reprecipitation from hexane and washing with diethyl ether and methanol. The products were isolated in the form of fibrous or powdery precipitates with metallic luster depending upon the length of the alkyl side chains. Solubility of these polymers was largely dependent on their substitution patterns. Interestingly, elongation of the *N*-alkyl side chain showed enhanced solubility of the polymers in organic solvents such as dichloromethane, chloroform, tetrahydrofuran, and toluene when compared to the elongation of the *O*-alkyl side chains.

FT-IR spectra of **6a**−**g** showed a strong peak between 1620 and 1630 cm^{-1}, which is characteristic of a resonance stabilized 1,3-cyclobutanediolate dianion moiety of the squaraine chromophore. ^{1}H NMR spectra of the soluble polysquaraines in $CDCl_3$ showed broad peaks corresponding to the aromatic protons, indicating a strong aggregation of the rigid conjugated polymer backbone. For a better insight into the structure of the polymers, the intermediate compounds **7a** and **7g** were prepared by the reaction of **5a** and **5g** with squaric acid in a 2:1 stoichiometry under high dilution and characterized by high-resolution mass spectra and ^{1}H NMR analyses (see Supporting Information). To further establish the structure of the polysquaraines, **6a** and **6g** were independently prepared by the reaction of **7a** and **7g** with squaric acid (1:1 stoichiometry) as shown in Scheme 2 (route B). Spectral properties of the polysquaraines prepared through routes A and B were identical. Elemental analysis revealed the presence of a molecule of water for every repeating unit of the polymers.[20] Thermogravimetric analysis (TGA) of **6a**−**g** under nitrogen atmosphere showed a minor weight loss between 150 and 250 °C, which could be due to the adsorbed water molecules and a major weight loss between 300 and 500 °C due to the degradation of the side chains and the backbone (see Supporting Information). As expected, the polysquaraines with short alkyl side chains showed relatively better thermal stability when compared to those with long side chains.

Size exclusion chromatography (SEC) of the soluble polysquaraines, which were prepared under different experimental conditions showed considerable differences in the retention times and molecular weights. For

(19) (a) Treibs, A.; Jacob, K. *Angew. Chem.* **1965**, *77*, 680. (b) Schmidt, A. H. *Synthesis* **1980**, 961. (c) Law, K. Y. *Chem. Rev.* **1993**, *93*, 449 and references therein.

(20) Elemental analysis was also performed after heating the polymers above 100 °C for several hours, which provided values close to the structures without water molecules. However, reasonable values within the error limits could not be obtained, which indicate that complete removal of the water molecules is not possible. We prefer to report the elemental analysis values of the polymers as obtained because, the reported properties correspond to those structures.

Table 1. GPC Data of the Soluble Polysquaraines 6d−g

polymer	R	R′	M_n	M_w	M_w/M_n[a]
6d	$C_{12}H_{25}$	CH_3	15827	124346	7.9
6f	$C_{12}H_{25}$	C_8H_{17}	17700	181131	10.2
6g	$C_{12}H_{25}$	$C_{12}H_{25}$	28450	307260	10.8

[a] The observed high polydispersities indicate aggregation of the polymer chains. Detailed investigation of the aggregation and photophysical behavior of these polymers are in progress.

Table 2. Solution and Solid-State Optical Properties of the Polysquaraines 6a−g

	solution[a]			solid state[b]		
polymer	λ_{max}[c] (nm)	λ_{onset}[d] (nm)	E_g[e] (eV)	λ_{max}[c] (nm)	λ_{onset}[d] (nm)	E_g[e,f] (eV)
6a	871, 1041	1300	0.95	880	1570	0.79
6b	870, 1022	1220	1.02	875	1530	0.81
6c	850, 1020	1225	1.01	860	1500	0.82
6d	870, 978	1170	1.06	870, 1028	1390	0.89
6e	890, 985	1140	1.09	890, 1020	1250	0.99
6f	882, 998	1160	1.07	905, 1025	1208	1.02
6g	868, 975	1140	1.09	881, 1021	1215	1.02

[a] In dichloromethane. [b] Film cast from chloroform solution. [c] Long wavelength values correspond to shoulders of varying intensity except in the case of **6e** and **6f**. [d] Determined by drawing a tangent from the long wavelength shoulder to λ_{0-0}. [e] Calculated from the onset of absorption. [f] ± 0.02 eV.

example, samples collected at different intervals from the reaction of **6g** and squaric acid showed an increase in molecular weights and dispersity with time. All soluble polysquaraines under investigation showed considerable broadening of the elution bands with more than one maximum even after repeated purification of the polymers. The weight average molecular weights and polydispersities obtained in these cases were unexpectedly high, which could be due to their strong tendency for aggregation in solution.[21] The number average molecular weights (M_n) of **6d**, **6f**, and **6g** were around 15827, 17700, and 28450 g/mol with polydispersities around 7.9, 10.2, and 10.8, respectively (Table 1). For a comparison, a model compound **7g** of known molecular weight of 2007 g/mol was subjected to SEC, which showed a sharp (major) elution peak with molecular weight of 3142 g/mol and a broad (minor) band corresponding to a molecular weight of 4824 g/mol. Since these values are higher than its actual molecular weight, we conclude that the observed weight average molecular weights and the polydispersities of the polymers are much higher than their actual values.[22]

Electronic Absorption Spectral Properties. The UV−Vis−NIR absorption spectral data of **6a−g** in toluene are summarized in Table 2, which revealed several interesting features that are unique to the new polymers. The absorption spectra of the polysquaraines **6a−g** and the model compound **7g** are shown in Figure 1. The model compound **7g** showed a sharp and intense

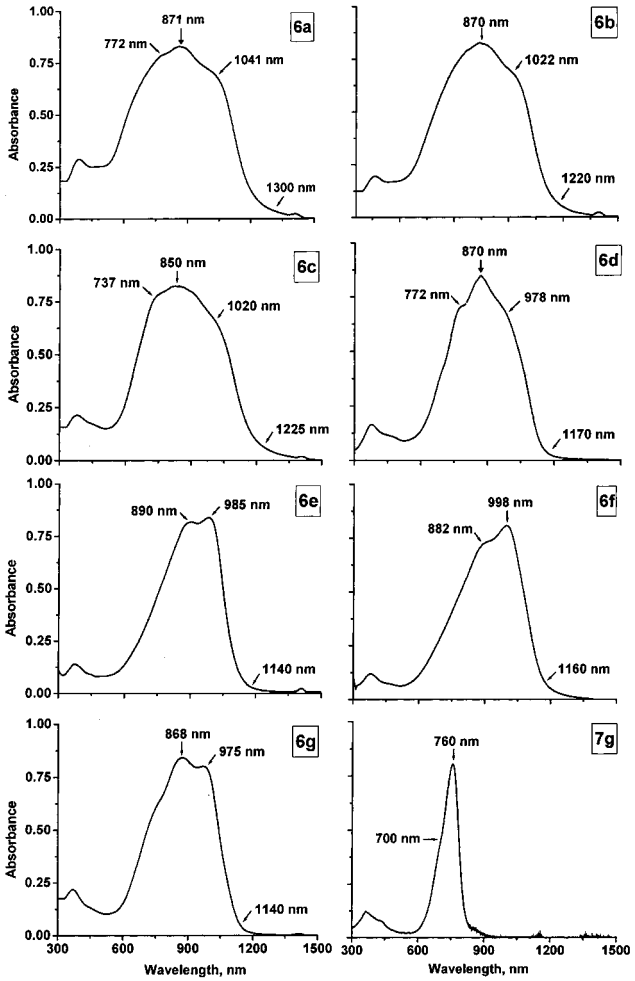

Figure 1. UV−Vis−NIR spectra of **6a−g** and **7g** in toluene.

Chart 1

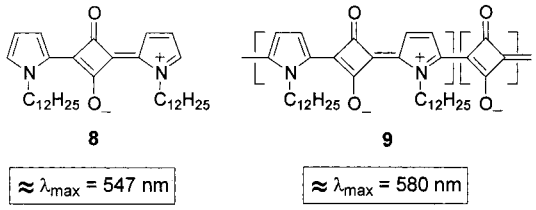

absorption maxima around 760 nm, which is characteristic of squaraine dyes, due to the small Franck−Condon factors for higher vibrational states associated with their rigid structures. The shoulder band at 700 nm is common to many squaraine dyes and could be attributed to exciton interaction.[23] The observed red shifts of 213 nm for **7g** when compared to the absorption maximum of the earlier reported squaraine dye **8** (Chart 1) is in agreement with some of the earlier reports that the optical properties of squaraine dyes are tunable by extending their conjugation length or by introducing electron donor moieties.[24] However, it is important to note that, despite the extended conjugation, poly-

(21) Aggregation is postulated also based on our preliminary information on solvent and temperature dependent changes in the absorption spectra. Detailed studies are in progress and will be published elsewhere.

(22) Molecular weight analysis of rigid conjugated polymers using flexible polystyrenes as standards has several limitations. It is reported that the observed molecular weights of rigid polymers in several cases are much higher, typically by a factor of 2−3, than the absolute value. (a) Grell, M.; Bradley, D. D. C.; Long, X.; Chamberlain, T.; Inbasekaran, M; Woo, E. P.; Soliman, M. *Acta Polym.* **1998**, *49*, 439. (b) Huang, S. L.; Tour, J. M. *J. Am. Chem. Soc.* **1999**, *121*, 4908. (c) Tour, J. M. *Chem. Rev.* **1996**, *96*, 537.

(23) Liang, K.; Farahat, M. S.; Perlstein, J.; Law, K.-Y.; Whitten, D. G. *J. Am. Chem. Soc.* **1997**, *119*, 830.

(24) (a) Chen, C.-T.; Marder, S. R.; Cheng, L.-T. *J. Am. Chem. Soc.* **1994**, *116*, 3117. (b) Meier, H.; Dullweber, U. *Tetrahedron Lett.* **1996**, *37*, 1191. (c) Meier, H.; Dullweber, U. *J. Org. Chem.* **1997**, *62*, 4821. (d) Meier, H.; Petermann, R.; Gerold, J. *Chem. Commun.* **1999**, 977. (e) Meier, H.; Petermann, R. *Tetrahedron Lett.* **2000**, *41*, 5475.

Scheme 3

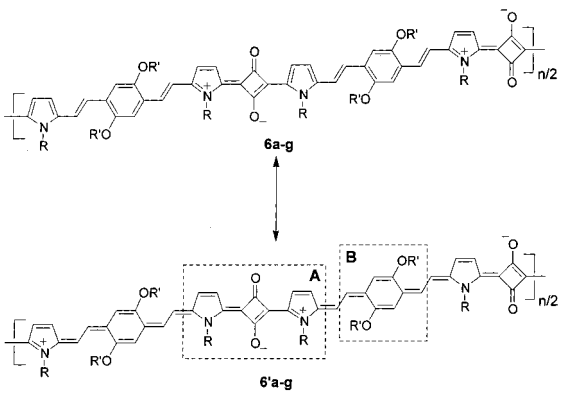

squaraine **9** could show only a marginal red shift of 33 nm from the absorption maximum of the dye **8,** which reveals that the S_0-S_1 transition is largely localized on the central cyclobutane ring. This can be rationalized on considering that each squaraine units in **9** is bridged through an electron deficient cyclobutane moiety thereby considerably weakening the charge-transfer interaction.

Since the ground-state S_0 as well as the first excited singlet state S_1 of squaraines represent intramolecular charge transfer states of donor−acceptor−donor type interaction, we anticipated that introduction of a strong conjugated electron donor bridge will substantially change the absorption properties of the resulting polysquaraines. Further, we speculated that the positive charge on the zwitterionic dye moieties could be delocalized along the conjugated backbone, thus generating planar and rigid quinoid resonance structures **6′a**−**g** as shown in Scheme 3. The broad and red shifted NIR absorptions of **6a**−**g** between 600 and 1200 nm in comparison to the sharp absorption of **7g** support the above arguments. The vibronic features of the absorption spectra are an indication of a relatively rigid and planar polymer backbone with high degree of conjugation. The intense NIR absorption of the new polysquaraines is striking in the sense that the designing of such π-conjugated polymers is rather difficult due to the decrease in the effective conjugation length (ECL) upon the polymer chain extension which is associated with conformational disorders.[25] Comparison of the UV−Vis−NIR absorption spectra of **6a**−**g** (Figure 1) reveals that the absorption maxima and the vibronic features are significantly influenced by the length of the hydrocarbon side chains. For example, **6a**−**c** with *N*-methyl group showed broad absorption between 600 and 1200 nm, whereas **6e**−**g** with *N*-dodecyl group showed relatively narrow spectra with 50−60 nm blue shifted absorption with considerable differences in the ratio of the intensities of the shoulder bands. The noted difference in the absorption spectra of these polymers is that the spectral region around 700 nm is more intense in **6a**−**c** when compared to those of **6d**−**g**. This could be due to an enhanced exciton coupling due to polymer backbone interaction in **6a**−**c**, which is associated with the relatively rigid and planar conformation. The solution E_g of **6a**−**g** were calculated from the onset of their absorption band, which revealed that those

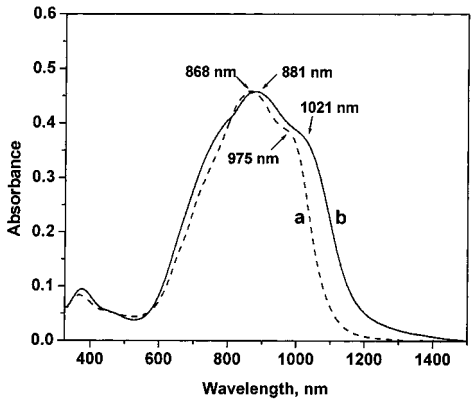

Figure 2. Comparison of the solution (a) and solid-state (b) absorption spectra of polysquaraine **6g**.

polymers with *N*-methyl groups show relatively low E_g when compared to those with *N*-dodecyl groups (Table 2). These values are much lower than the solution E_g of many of the reported zwitterionic and donor−acceptor polymers. The lowest solution E_g of 0.95 eV was obtained for **6a** with *N*-methyl and *O*-butyl side chains.

Solid-State Electronic Absorption Properties. The solid-state (film) absorption maxima, onset of absorption, and the corresponding band gaps of **6a**−**g** are summarized in Table 2. In general, the electronic properties such as absorption and emission of conjugated polymers are considerably different in the solid-state when compared to their solution behavior. This is mainly due to the formation of well-ordered self-assemblies of the macromolecular backbone in the solid-state as demonstrated in the case of poly(*p*-phenyleneethynylene)s[26] and regioregular poly(3-alkylthiophenes).[27] Interestingly, although the solid-state absorption spectral features of the new polysquaraines are more or less identical to their solution spectra, a marginal red shift of the absorption maxima and broadening on both shorter as well as the longer wavelength regions could be seen as shown in the case of **6g** (Figure 2). It is likely that these marginal changes of the solid-state absorption spectrum could be due to a more specific and ordered packing of the aggregates of the polymer chains in the solid film. The solid-state band gaps of **6a**−**g** were calculated from the onset of the solid-state (film) absorption spectra, which are 0.1−0.2 eV less, when compared to the band gaps calculated from the onset of the solution absorption spectra (Table 2).[28]

Electrochemical Properties. The cyclic voltammograms of the soluble polysquaraines **6e**−**g** in dichloromethane using tetrabutylammonium hexafluorophosphate as the supporting electrolyte showed broad redox bands probably due to their polydisperse nature and the intrinsic aggregation behavior (see Supporting Information). Several electrochemical processes may be occurring simultaneously, and hence we could not obtain the

(25) Meier, H.; Stalmach, U.; Kolshorn, H. *Acta Polym*. **1997**, *48*, 379.

(26) (a) Bunz, U. H. F. *Chem. Rev*. **2000**, *100*, 1605. (b) Halkyard, C. E.; Rampey, M. E.; Kloppenburg, L.; Studer-Martinez, S. L.; Bunz, U. H. F. *Macromolecules* **1998**, *31*, 8655.

(27) McCullough, R. D.; Lowe, R. D.; Jayaraman, M.; Anderson, D. L. *J. Org. Chem*. **1993**, *58*, 904.

(28) E_g determined from the onset of the broad absorption of the polymer film is strongly influenced by the mode of preparation and the thickness of the film. Hence, there may be some error in estimation of these values. On the other hand, the E_g determined from the onset of the solution spectra are more accurate.

Table 3. XRD and Conductivity Data of Polysquaraines 6a−g

polymer	d_1 (Å)	d_2 (Å)	d_3 (Å)	intrinsic conductivity (S/cm)[a]	doped conductivity (S/cm)[b]
6a	11.0	5.3	3.4	5.3×10^{-4}	5.20×10^{-2}
6b	14.7	4.6	3.4	8.75×10^{-4}	2.98×10^{-2}
6c	19.2	4.6	3.4	4.21×10^{-6}	6.17×10^{-2}
6d	17.0	4.4	3.8	2.20×10^{-5}	1.10×10^{-2}
6e	18.4	4.2		4.40×10^{-6}	2.80×10^{-2}
6f	20.5	4.3		6.20×10^{-6}	5.10×10^{-2}
6g	21.0	4.5		6.30×10^{-7}	1.10×10^{-2}

[a] Measured on pressed bars using two probe methods (Kiethley model 6517A electrometer). [b] Measured after exposure in iodine until a constant weight is obtained.

peak potential separation. However, multisweep experiments showed good reversibility of the electrochemical processes. In contrast, the model compound **7g** showed an irreversible cyclic voltammogram with two oxidation peaks ($E^1_{ox} = 0.87$ V, $E^2_{ox} = 1.4$ V). Repeated scanning of **7g** showed the growth of a polymer film on the electrode due to the oxidative polymerization of the pyrrole end groups. UV−Vis−NIR spectroelectrochemical analysis of **6g** under various applied potentials showed a gradual decrease of their absorption maxima around 850 nm with concomitant growth of a broad absorption at the NIR region indicating the oxidation of the polymer backbone (see Supporting Information).

X-ray Diffraction Studies. Insight into the molecular level ordering of **6a−g** was obtained from their powder X-ray diffraction patterns. These patterns showed interdigitated morphology with three-dimensional ordering of the polymer backbone as reported in the case of certain poly(phenyleneethylene)s.[26,29] Elongation of the hydrocarbon side chain and their substitution patterns have a significant influence on the molecular packing as evident from the comparison of the XRD data of **6a−g** (Table 3). Among **6a−c,** the interchain packing distance increased from 11 to 19.2 Å upon elongation of the side chain from *O*-butyl to *O*-dodecyl, while the interlayer π-stacking distance of 3.4 Å at the wide-angle region remained nearly the same and independent of the variation of the side chain length. At the same time, a new diffraction pattern corresponding to a distance of 4.6 Å appeared, indicating two types of interlayer packing probably due to the slipping of the stacked layers. Surprisingly, in the case of **6d−g** with *N*-dodecyl groups, the interlayer packing distances of 3.4 and 4.6 Å merged to a broad band corresponding to a distance of 4.2−4.5 Å, indicating considerable disruption of the stacking. This is clear from the comparison of the XRD patterns of **6a**, **6c**, **6d**, and **6f** having different side chains as shown in Figure 3. These observations imply that elongation of the *N*-alkyl chains has considerable influence on both the interchain as well as interlayer packing of the polysquaraines, whereas elongation of *O*-alkyl chains has influence mainly on the interchain packing.

For a better understanding of the molecular ordering of the squaraine polymers, their interchain packing distances were compared with those of the regioregular

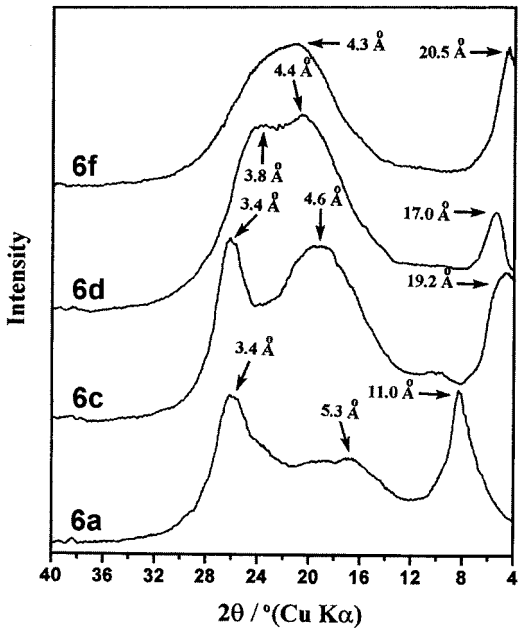

Figure 3. XRD patterns of polysquaraines **6a**, **6c**, **6d**, and **6f**.

polythiophenes which are reported to form lamellar packing.[30] The reported interchain spacing of a regioregular poly(3-butylthiophene) is 12.63 Å and that of a poly(3-dodecylthiophene) is 27.19 Å. However, these distances of polysquaraines with butyl and dodecyl side chains are 11.0 and 19.2 Å, respectively, which are nearly 1.6 and 8.0 Å less when compared to those of analogous polythiophenes. The interchain distance of **6g** which has *N*- and *O*-dodecyl side chains is around 21.0 Å, which is again 6 Å less than a regioregular poly(3-dodecylthiophene). These studies suggest an interdigitated comblike arrangement of the alkyl chains for the polysquaraine with a probable slipped stacking to maximize the electrostatic interactions as shown in Figure 4. This can be supported by the molecular modeling studies of the model compound **7g** (TITAN version 1, MM force field). The calculated interchain distance of the minimum energy conformation of **7g** for end-to-end lamellar packing is 35 Å, whereas the interdigitated packing distance is 17 to 18 Å. The observed interchain packing distance of an analogous polysquaraine **6g** is 21 Å, which is very close to the calculated interdigitated packing distance. In all cases, the observed interchain *d*-spacing was much shorter than the calculated values, indicating an interdigitated packing, which however varied with the length of the alkyl side chains.

Scanning Electron Microscopy (SEM). To have a physical picture of the morphology of the polysquaraines, films of two representative samples **6d** and **6g** were subjected to the SEM analysis. These pictures reveal considerable morphological differences between the two polymers. Figure 5A corresponds to the SEM photograph of **6d** with *O*-methyl and *N*-dodecyl side chains, which shows the presence of aggregated microcrystalline domains. On the other hand, the SEM picture of the polymer **6g** with *O*-dodecyl and *N*-dodecyl side chains

(29) (a) Li, H.; Powell, D. R.; Hayashi, R. K.; West, R. *Macromolecules* **1998**, *31*, 52. (b) Moroni, M.; LeMoigne, J.; Luzzati, S. *Macromolecules* **1994**, *27*, 562.

(30) (a) McCullough, R. D.; Tristram-Nagle, S.; Williams, S. P.; Lowe, R. D.; Jayaraman, M.; *J. Am. Chem. Soc.* **1993**, *115*, 4910. (b) Chen, T. -A.; Wu, X.; Rieke, R. D. *J. Am. Chem. Soc.* **1995**, *117*, 233.

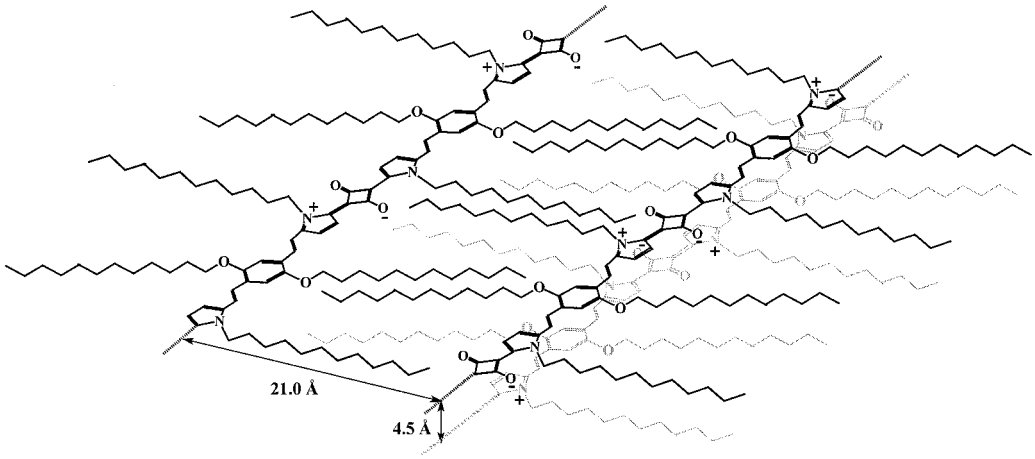

Figure 4. Interdigitated molecular packing diagram of polysquaraine **6g.** The calculated *d*-spacing value for the interdigitated packing of **6g** is 17.6 Å, whereas the observed value is 21.0 Å (TITAN version 1, MM force field).

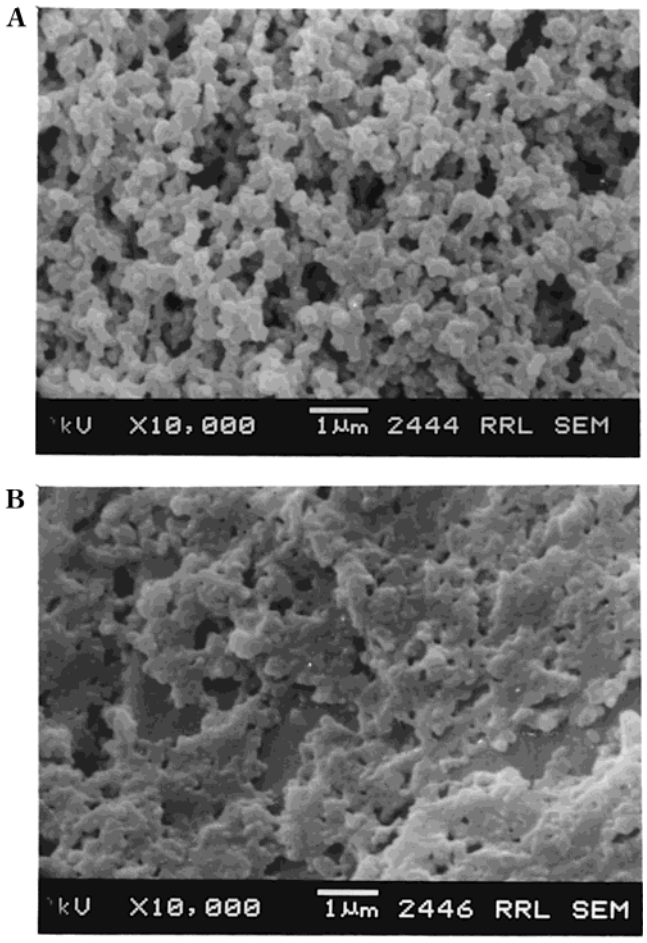

Figure 5. SEM pictures of **6d** (A) and **6g** (B).

revealed an amorphous morphology of the agglomerated aggregates (Figure 5B).

Conductivity. The intrinsic and doped electrical conductivities of the polysquaraines **6a**−**g** are listed in Table 3, which are in agreement with the molecular packing data obtained from the XRD studies. It is known that the ordered domains present in the self-organized microstructures of π-conjugated polymers have a crucial role in their charge carrier mobility and photopysical properties.[31] In such cases, the interchain electron hopping will become efficient, which in turn will enhance the electrical conductivity. The data from the conductivity measurements of **6a**−**g** are consistent with the XRD analysis, which is in support of the proposed molecular packing. As shown in Table 3, the intrinsic conductivities could be varied from 10^{-7}−10^{-4} S/cm by varying the length of the alkyl side chains. The highest conductivities were in the order of 10^{-4} S/cm for **6a** and **6b** with short side chains, whereas the conductivity decreased gradually with elongation of the side chains. The lowest conductivity (6.3×10^{-7} S/cm) was observed for **6g** with *N*- and *O*-dodecyl chains. Even though the band gaps of **6a**−**g** are reasonably low in all the cases, considerable difference in their conductivity could be seen indicating that molecular packing has a more decisive role than the band gaps in determining the conductivity in these polymers. The higher conductivity of **6a** and **6b** could be due to an efficient electron hopping process, which is facilitated by the close interchain packing and the short interlayer π-stacking. Decrease in the conductivity with steady elongation of the side chain is due to the disruption of the π-stacking by the increased *d*-spacing within the layered assemblies. In all cases, exposure of the sample in iodine vapors enhanced the conductivity, which reached a limiting value in the order of 10^{-2} S/cm.

Even though we cannot unequivocally rule out the possibility of any adventitious doping by atmospheric oxygen, the extent of such doping, if there is any, would be minimal since we could not observe any considerable change in the absorption spectra even after bubbling of oxygen to the solutions of the freshly prepared polysquaraines. A comparison of the absorption spectra of the polysquaraines before and after the conductivity measurement did not show any considerable change in the nature of the absorption bands. On the other hand, addition of iodine to a solution of these polymers considerably reduced the intensity of their characteristic absorption bands with the formation of a broad band between 1200 and 1500 nm through an isosbestic point at 1111 nm (Figure 6). The sharp absorption around 500 nm could be due to residual iodine. This observation is

(31) (a) Sirringhaus, H.; Brown, P. J.; Friend, R. H.; Nielsen, M. M.; Bechgaard, K.; Langeveld-Voss, B. M. W.; Spiering, A. J. H.; Janssen, R. A. J.; Meijer, E. W.; Herwing, P.; de Leeuw, D. M. *Nature* **1999**, *401*, 685. (b) McQuade, D. T.; Kim, J.; Swager, T. M. *J. Am. Chem. Soc.* **2000**, *122*, 5885.

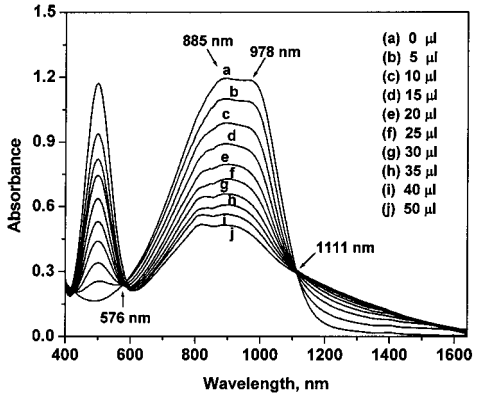

Figure 6. Changes in the absorption spectrum of **6e** in toluene upon addition of iodine solution (0.07 M in toluene).

comparable to the spectroelectrochemical changes of **6e**, which indicate that the oxidized species in both cases might be the same.

Conclusions

Strengthening of the donor−acceptor interactions, along with increasing the conjugation length is a convenient approach to modulate the electronic absorption properties of polysquaraines toward low optical band gap region. We have successfully illustrated this approach in the design of a series of extremely low E_g polysquaraines with intense NIR absorption. Incorporation of an electron-rich 2,5-dialkoxydivinylbenzene as bridging unit between squaraine moieties showed remarkable influence in altering the optical and electronic properties of the resulting polysquaraines. The structured NIR absorption spectra of the new polysquaraines suggest a high degree of conjugation and planarization of the polymer backbone. The onsets of absorption of **6a**−**g** in solution are unusually high, and the band gap obtained for these polymers is one of the lowest ever reported, when compared to several of the known conjugated polymers. Length of the alkyl side chain has considerable influence on the optical and conducting properties. The present study demonstrates the use of an organic dye to design low E_g donor−acceptor-type polymers and the modulation of their optical and electronic properties by the logical selection of their molecular components. Conjugated polymers with such intense NIR absorption and low optical band gaps are rare in the literature.

Acknowledgment. We thank Dr. U. Syamaprasad and Dr. Peter Koshy for XRD and SEM analyses, respectively. We are grateful to Mr. V. P. Balagangadharan, Analytical and Spectroscopy Division, VSSC, Trivandrum for the help with GPC analysis. Spectroelectrochemical data provided by Professor Dr. Jöerg Daub and Dipl. Chem. Michael Büschel, University of Regensburg, Germany, are gratefully acknowledged. This work was supported by the Department of Science and Technology (DST Grant-in-aid No. SP/S1/G-11/97) and the Council of Scientific and Industrial Research, Government of India (SRF to J.E.). This is manuscript no. RRLT-PRU-141.

Supporting Information Available: Synthesis and characterization of **2a**−**c**, **3a**−**d**, **4a**−**d**, and **7a**, **g**. The evolution of absorption spectra of polysquaraines **6a** and **6f** with time. TGA plots of **6c**, **6d**, and **6g**. Cyclic voltammograms of **6g** and **7g** and the spectroelectrochemical data of **6g** (PDF). This material is available free of charge via the Internet at http://pubs.acs.org.

CM0107225